Snodar: An acoustic radar for atmospheric turbulence profiling with 1m resolution

C. S. Bonner[1*]**, M. C. B. Ashley**[1]**, J. S. Lawrence**[1,2,3]**, D. M. Luong-Van**[1]**, J. W. V. Storey**[1]

[1] **School of Physics, The University of New South Wales, NSW 2052, Australia**
[2] **Department of Physics and Engineering, Macquarie University, NSW 2109, Australia**
[3] **Anglo-Australian Observatory, NSW 1710, Australia**

[*]cbonner@phys.unsw.edu.au

ABSTRACT: Snodar is a 5 kHz monostatic acoustic radar designed to measure the atmospheric turbulence within the first 200 m of the atmosphere with a vertical resolution of 1 m. An in situ calibration target is used to give absolute intensity calibration. The primary motivation for building Snodar is to quantify the site conditions for a future astronomical observatory in Antarctica. Two Snodar instruments are operating at Dome A, Antarctica, during 2009 as part of the completely robotic "PLATO" facility. The instruments are separated by 20 m and sample from 8 m to 200 m with a resolution of 1 m allowing the spatial and temporal characteristics of the atmospheric boundary layer to be investigated. We present here the acoustic design of Snodar and example data demonstrating the performance of the instrument.

1. INTRODUCTION

Optical observations of astronomical objects made from ground-based observatories are hampered by the Earth's atmosphere. This is primarily due to turbulent mixing within the atmosphere causing temperature fluctuations, and hence variations in the refractive index, resulting in "optical turbulence". This causes stars to no longer appear as point sources, a phenomenon that astronomers refer to as *seeing*, and limits the resolving power of large optical telescopes. The characteristics of the optical turbulence at a given site is of major importance in deciding whether to build an observatory there.

Optical turbulence is generally confined to the lowest 20 km of the Earth's atmosphere, with a dramatic increase within the lowest 1 km due to the direct interaction of the atmosphere with the Earth's surface. The lower layer is called the atmospheric boundary layer, and its height is dependent on the local topography, the surface roughness, and the surface energy budget, which in turn depends on the position of the sun, cloud coverage, surface type, and other factors. The portion of the atmosphere above the atmospheric boundary layer is called the free atmosphere.

Harper [1] and Gillingham [2] made early predictions that Antarctica could be a favorable location from which to make astronomical observations. Dome C, at a height of 3233 m on the Antarctic plateau as shown in Figure 1, has been shown to have exceptional free-air seeing [3]. Subsequent experiments at Dome C have shown that ∼90% of the total optical turbulence is confined within a shallow atmospheric boundary layer with a typical height of 30 m [4]. This result is very promising for astronomers as it is technically feasible to place a 2 m class optical telescope on a 30 m tower [5][6]. Such a telescope could have a comparable resolving power to the Hubble Space Telescope for a useful percentage of the time. The plateau observatory, PLATO, has been designed to assess the potential of Dome A, the highest location on the Antarctic plateau, as an astronomical observatory [7]. Designed at
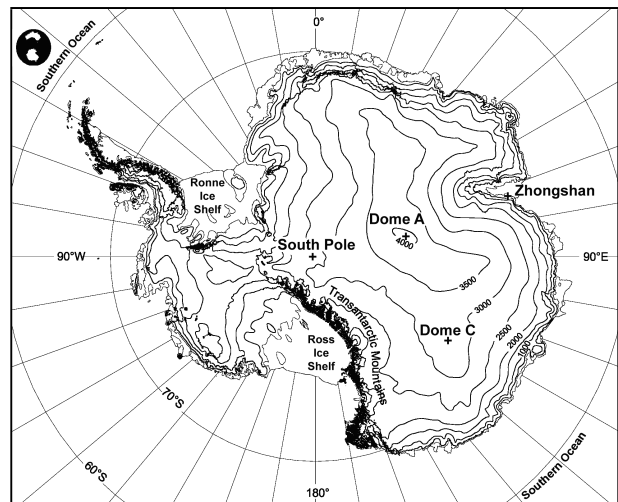
Figure 1. Map of Antarctica showing the South Pole, Dome C and Dome A. Basic map courtesy of the Australian Antarctic Data Center.

the University of New South Wales, PLATO was deployed to Dome A in January 2008 by the National Astronomical Observatories of the Chinese Academy of Sciences and the Polar Research Institute of China. One of the key science goals for PLATO is to characterize the height and variability of the atmospheric boundary layer.

Several techniques have been developed to remotely measure optical turbulence, e.g. [8][9]. Of these, acoustic radars (or SODARs) have the advantage of relatively high spatial and temporal resolution. However, acoustic radars are non-trivial to calibrate and are normally used to profile 3-dimensional wind speed within the first 2 km of the atmosphere. Typical commercial SODARs also only have a vertical resolution of approximately 10 m.

No commercial instruments are available to profile the first 100 m of the atmosphere to a resolution of 1 m or better, which

1

is what is needed on the Antarctic plateau. For this reason we developed Snodar. Snodar is a robust, autonomous, high-resolution turbulence profiling acoustic radar that can operate down to temperatures of $-80°$C. We describe here the theoretical background, acoustic design and performance of Snodar. The electrical design of Snodar has been published by Bonner et al. [10][11] while initial results from PLATO have been published by Yang et al. [12], and Ashley et al. [13].

2. THEORETICAL BACKGROUND

In 1941 Andrey Kolmogorov developed theories [14] that allowed the chaotic phenomenon of turbulence to be described statistically for very high Reynolds numbers. Simply put, the Kolmogorov theory of turbulence states that energy enters a turbulent field at some outer length scale L_0 and is redistributed into smaller and smaller scales by eddy action until some inner scale l_0 is reached. Energy enters the turbulent field at L_0 due to variations in the average wind velocity and leaves the field at l_0 as heat due to molecular viscosity. Eddies with length scales of L where $l_o \ll L \ll L_o$ are said to be in the inertial range. Turbulence within the inertial range is ideally homogenous and isotropic. Tatarskii [15] shows that structure functions can be used to describe turbulent fields. The structure function for turbulence within the inertial range of fully developed turbulence obeys the $\frac{2}{3}$ law from Kolmogorov and Obukhov [15] and is defined as

$$D(\mathbf{r}) = C^2 \varepsilon^{\frac{2}{3}} \mathbf{r}^{\frac{2}{3}} \tag{1}$$

where ε is the energy dissipation rate and C is the structure function constant for the parameter of interest. A structure function constant can be physically interpreted as the mean squared difference of some parameter between points throughout the turbulent field and describes the intensity of the turbulence. The refractive index structure function constant C_N^2 is of primary interest to astronomers as astronomical seeing is proportional to the three-fifths power of the integral of C_N^2 along the line of sight [15]. Tatarskii also shows that the temperature structure function constant C_T^2 can be related to the optical refractive index structure function constant C_N^2.

Temperature and velocity inhomogeneities caused by turbulence within a medium on the scale of $\lambda/2$ are responsible for scattering acoustic waves with a wavelength λ. The acoustic scattering cross-section σ of a turbulent volume is a function of the temperature and velocity structure function constants, C_T^2 and C_V^2 respectively. The scattering cross-section is the scattered power per unit area per incident power per unit volume having dimensions $m^2 m^{-3}$ and is given by [15]

$$\sigma = 0.03 \left(\frac{\omega}{c(h)} \right)^{\frac{1}{3}} cos^2\theta \left[\frac{C_V^2}{c(h)^2} cos^2\frac{\theta}{2} + 0.13 \frac{C_T^2}{T(h)^2} \right] \left(sin\frac{\theta}{2} \right)^{\frac{-11}{3}} \tag{2}$$

where ω is the frequency of the acoustic wave in radians per second, θ is the scattering angle relative to the original wave vector, T is the average temperature of the scattering volume and $c(h)$ is the speed of sound at height h. It can been seen by examining Equation 2 that if $\theta = \pi$ then σ is only dependent on C_T^2 i.e. if a monostatic system—one with a collocated trans-

mitter and receiver—is used, then the back scatter is solely a function of the temperature structure function constant.

Little [16] first proposed using acoustic radars, or SODARs, to probe the structure of the Earth's lower atmosphere in 1969. Little demonstrated that the acoustic power received at an antenna is related to the scattering cross-section by the SODAR equation

$$P_R = P_T \eta A \sigma \frac{c(h)\tau}{2} \frac{e^{-2\alpha h}}{h^2} \tag{3}$$

where h is the height of the turbulent volume with a scattering cross-section of σ, τ is the pulse duration, η is the system gain, α is the atmospheric attenuation constant and P_T and P_R are the power transmitted and the power received by the antenna's effective area A. Therefore the contribution to astronomical seeing can be calculated from the scattered acoustic energy received by a monostatic acoustic radar after correcting for atmospheric attenuation and the system gain. The process of determining the system gain, or calibrating the instrument, is non-trivial and will be discussed in Section 4. It is worth noting that P_R/P_T is typically on the order of 10^{-15}.

Snodar is an acoustic radar and works by sending an intense acoustic pulse into the atmosphere and recording the faint backscatter off the atmospheric turbulence. The vertical resolution $\triangle h$ of an acoustic radar is

$$\triangle h = \frac{c(h)\tau}{2} \tag{4}$$

The height h of the scattering volume is a function of the time of flight t and the speed of sound along the acoustic path and is given by solving

$$h(t) = \frac{1}{2} \int_0^t c(h) dt \tag{5}$$

The minimum sampling height of an acoustic radar is limited by transducer ringing, antenna reverberation or echoes from fixed objects, also called ground clutter. The minimum sampling height for commercial units is typically 20~40 m. Such commercial units are not useful when investigating a shallow atmospheric boundary layer $\leq$30 m in height.

3. ACOUSTIC DESIGN

Snodar was designed to investigate the atmospheric boundary layer on the high Antarctic plateau throughout the polar year. To accomplish this, Snodar must 1) have a vertical resolution of 1 m or better, 2) have carefully controlled transducer ringing and antenna reverberation to allow sampling within 10 m of the ground, 3) operate fully autonomously, and 4) have a well-determined absolute intensity calibration throughout the polar year. The requirement of maintaining intensity calibration posed a considerable design challenge due to wide ambient temperature range of $-80°C$ to $-30°C$ and the requirements of completely robotic operation. Calibration of the instrument will be discussed in Section 4. The acoustic design of the instrument will be discussed in this Section.

The nominal operating frequency of an acoustic radar is the prime design decision as it determines the scale of the antenna and possible transducers. The optimal operating frequency can be found by looking for the maximum in Equation

3 with respect to ω after substituting for σ from Equation 2. Interestingly, acoustic energy propagates exceedingly well in Antarctica due to the extreme cold. For example, the attenuation at 5 kHz at normal room temperature with 50% relative humidity is about 40 dB/km, whereas at $-60°$C the attenuation is only 4 db/km [17]. The attenuation increases to about 16 dB/km at Dome A due to the reduced atmospheric pressure at this elevation (4091 m). The optimal operating frequency for Snodar was found to be 5 kHz. A transmitted pulse duration of 33 cycles at 5 kHz provides a vertical resolution of 1 m.

Snodar uses a single transducer mounted near the focal point of a parabolic reflector to transmit an intense acoustic pulse and receive the faint backscatter. This makes Snodar a true monostatic acoustic radar. A $0.9m$ $f/0.6$ commercial parabolic satellite dish is used to collimate the acoustic energy generated by the transducer. The transducer we selected is a JBL2402H horn-loaded compression driver manufactured by JBL. The JBL2402H is rated for a continuous power of 40 W over a frequency range from 3 kHz to 15 kHz. The beam pattern generated by the antenna at 5 kHz is essentially diffraction limited with a beam width of $\approx 4°$. The reflector and transducer are housed in a 1.6 m tall 12-sided sound cone to reduce side lobes and acoustic noise. A cross-sectional view of the sound cone, reflector and transducer is shown in Figure 2. The sound cone consists of 12 separate panels and is flat-packable for easy transportation. The walls of the sound cone are tapered away from the acoustic beam at an angle of $8°$. The top surface of the parabolic reflector was aluminized
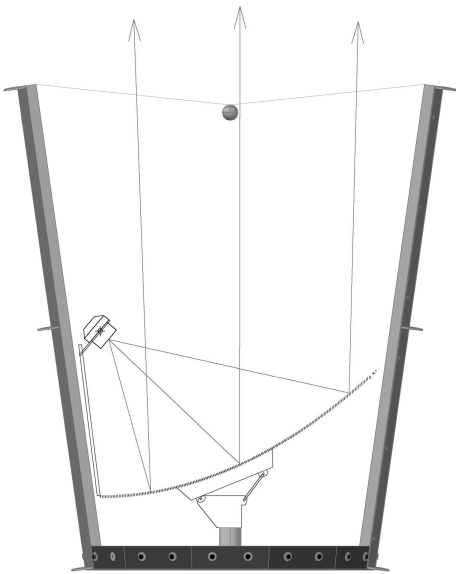
Figure 2. Cross-section of Snodar's 1.6 m tall antenna. The offset parabolic reflector and transducer are supported by a post at the bottom of the sound cone. The inside of the sound cone is lined with 50 mm of glasswool sound absorber. The calibration sphere, which is discussed in Section 4, is shown suspended across the antenna's aperture.

to reduce its thermal emissivity by approximately an order of magnitude. This allowed higher temperatures to be reached when heating the dish from electrical heat pads glued to its back surface. Heating was used to remove any accumulated snow. Focusing of sunlight by the aluminized reflector is not an issue while operating Snodar in polar regions as the sound cone ensures that the dish is always in shadow.

The inside of the sound cone is lined with 50 mm thick unfaced resin-bonded glasswool sound absorber. The sound absorber used is Quietel™ manufactured by CSR Bradford Insulation. A glasswool sound absorber was selected as fridge tests indicated that these materials maintain their acoustic properties down to $-80°C$ unlike many polymer-based sound absorbers which lose their acoustic properties and mechanical strength at sub-zero temperatures. Glasswool sound absorbers are also more suitable for long-term installation in direct sunlight.

The electronics that control Snodar are located inside the PLATO instrument module, which is kept above $-5°C$. A low-noise solid state switch and impedance-matching network are mounted close to the transducer in the sound cone to reduce the system's susceptibility to electromagnetic interference. The impedance-matching network is an important part of the system as it dramatically reduces transducer ringing. A WiFi based webcam has also been installed within the sound cone to visually monitor snow and ice accumulation.

4. INTENSITY CALIBRATION

The problem of calibrating the absolute intensity of SODARs is nontrivial and has been given considerable attention in recent decades [18]. For Snodar, we have the additional problems of coping with the wide operating temperature range of between $-30°C$ and $-80°C$, and the possible accumulation of snow and ice within the antenna. The variability of the speed of sound in air due to changes in the ambient air temperature can be corrected for during post-processing with data from automatic weather stations.

To maintain an absolute intensity calibration Snodar uses a calibration sphere made from solid phenolic resin (a billiard ball) suspended in the middle of the sound cone aperture, as shown in Figure 2. The calibration sphere provides a fixed echo with a known scattering cross-section at a known height. The positioning of the calibration sphere allows the gain of the system to be monitored and corrected for. A small amount of frost may form on the sphere, however the size and shape of the sphere is not expected to substantially change. The gain of the system however is expected to vary with transducer life, ambient temperature and accumulation of snow and ice on the parabolic reflector.

The scattering cross-section of the calibration sphere can be determined analytically, numerically or experimentally. Dragonette *et al.* [19] gives the acoustic scattering cross-section of spheres in the far field. Similar techniques could be applied to find an analytical solution for the scattering cross-section of Snodar's calibration sphere; however this is much more complicated as the sphere is in the near field of the antenna. Instead, Snodar is initially calibrated against tower-mounted microthermal sensors which measure C_T^2 directly; the scattering cross-section of the sphere is then found by comparing the echo from the sphere with the echo from turbu-

lence with known C_T^2. The sphere remains with Snodar allowing the instrument to be recalibrated without tower mounted instrumentation.

As the acoustic scattering from the calibration sphere is dependent on the acoustic wavelength which is dependent on ambient temperature, it is essential to calibrate Snodar at a range of wavelengths. A look-up-table of calibration constants as a function of wavelengths is generated during calibration allowing Snodar to be recalibrated at various ambient temperatures. Snodar currently recalibrates itself every 30 minutes at Dome A.

5. PERFORMANCE

Snodar was deployed to Dome A in 2008 as part of the PLATO facility [7]. During this first year we only obtained one week of data due to failure of the transducer diaphragm. However, these early results were promising since they clearly showed the expected diurnal cycle of the atmospheric boundary layer with an excellent signal-to-noise-ratio of up to 60dB. The 2008 instrument was repaired in 2009 and a second instrument was deployed. The two instruments are separated by 20 m and sample from 8 m to 200 m with a 1 m vertical resolution allowing the temporal and spatial characteristics of the atmospheric boundary layer to be investigated. Data are transmitted to Sydney Australia through the PLATO facility via the Iridium satellite network every 6 hours and stored in a MySQL database. The height of the atmospheric boundary layer is automatically extracted from the data and stored for statistical analysis.

The performance of the instrument can be seen with an echo from the 2008 data set. Figure 3 shows the received power as a function of scattering height for a single 5 kHz echo with a vertical resolution of 1 m; the height of the scattering volume is given by Equation 5. The raw signal was filtered to a bandwidth of 500 Hz centered at 5 kHz before the power was calculated with a moving average of the signal squared. The in-band transducer ringing/antenna reverberation is indicated by the straight line at approximately 5 m. The ringing/reverberation reduces to the noise floor at approximately 8 m. The signal power clearly deviates from $1/r^2$ at 40 m. Making the reasonable assumption that T is approximately constant around 40 m and that there is not a sudden increase in atmospheric attenuation above 40 m, Equation 3 indicates that there is a sharp drop in σ and therefore C_T^2, at a height of 40 m. This sudden drop in C_T^2 indicates the height of the atmospheric boundary layer. The power spectrum as a function of time (expressed as height via Equation 5) for the echo shown in Figure 3 is shown in Figure 4. The dark band within the first 5 m is due to spectral leakage from the intense initial pulse; the input signal was also being clipped within ± 1.4V for this period. Second and third order harmonics are also visible. The transducer's ringing is visible at its natural frequencies of 2.0 kHz, 2.5 kHz and 7.8 kHz. The natural frequencies of the transducer vary slightly with temperature but always remain outside the passband of the 4750 Hz to 5250 Hz digital filter. A Doppler shift is imparted on scattered waves if the velocity of the scattering surface or volume has a non-zero
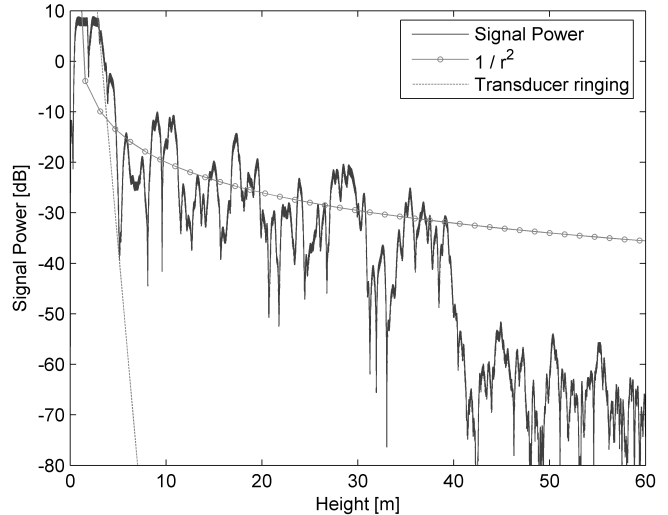
Figure 3. The first 60 m of a single 5 kHz echo from Snodar while operating at Dome A, Antarctica with a vertical resolution of 1 m. The raw signal was filtered to a bandwidth of 500 Hz centered at 5 kHz. The in-band transducer ringing/antenna reverberation is indicated by the straight line at approximately 5 m. $1/r^2$ is shown for comparison with Equation 3.

velocity component along the line of sight. This can sometimes be used to distinguish echoes from fixed objects and scattering from atmospheric turbulence, as the atmosphere is seldom stationary. This method, however, does not always allow antenna reverberation and scattering from turbulence to be separated for vertically pointed monostatic acoustic radars on the ground. This is because there is not always a vertical wind velocity several meters above the ground or within the antenna itself. Instead, Snodar uses linear frequency chirps and impulses of the form given in Equations 6 and 7 respectively where A_0 is the signal amplitude, ω is the chirp start frequency, α is the frequency sweep rate, δ is the Dirac-delta function. Linear frequency chirps and impulses are not efficiently scattered by turbulence which allows fixed echoes and antenna reverberation to be identified. This is only possible as Snodar has a wide operating range from 3 kHz to 15 kHz.

$$f(t) = A_0 sin((\omega + \alpha t)t) \qquad f(t) = A_0 \delta(t) \qquad (6,7)$$

6. CONCLUSION

We have presented here the acoustic design of a new instrument called Snodar designed specifically to profile atmospheric turbulence within the lowest 200 m of the Earth's atmosphere to a resolution of 1 m on the Antarctic plateau. The performance of the instrument has been demonstrated with actual data from Dome A, Antarctica obtained during 2008.

It is expected that the system gain will reduce with the accumulation of snow and ice within the antenna structure. The full impact of this will be assessed by comparing the system gain as determined by the in situ calibration sphere and the webcam images from within the sound cone throughout the polar year.
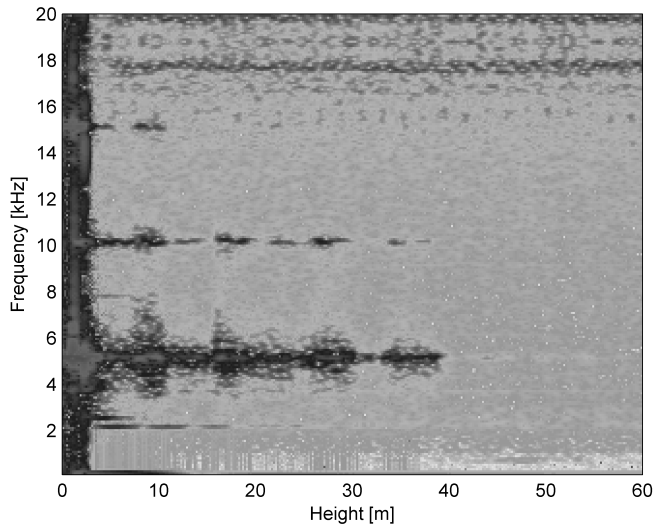
Figure 4. The power spectrum as a function of time (expressed as height via Equation 5) for the echo shown in Figure 3.

ACKNOWLEDGEMENTS

REFERENCES

[1] D.A. Harper D.A., "Infrared astronomy in Antarctica", *Astrophysics in Antarctica (A92-22401 07- 89). New York, American Institute of Physics*, 123-129 (1989)

[2] P.R. Gillingham, "Prospects for an Antarctic Observatory", *Proc. Ast. Soc. Aust.* **9**, 55–56 (1991)

[3] J.S. Lawrence, M.C.B. Ashley, A. Tokovinin, and T. Travoullion, "Exceptional astronomical seeing conditions above Dome C in Antarctica", *Nature* **431**, 278–281 (2004)

[4] E. Aristidi, E. Fossat, A. Agabi, D. Mékarnia, F. Jeanneaux, E. Bondoux, Z. Challita, A. Ziad, J. Vernin, H. Trinquet, "Dome C site testing: surface layer, free atmosphere seeing, and isoplanatic angle statistics", *A&A* **499**, 955–965 (2009)

[5] W. Saunders, P.R. Gillingham, A.J. McGrath, J.W.V. Storey, J.S. Lawrence, "PILOT: design and capabilities", *EAS Publications Series* **33**, 28–288 (2008)

[6] J.W.V. Storey, M.C.B. Ashley, M.G. Burton, J.S. Lawrence, W. Saunders, "PILOT-like telescope potential", *EAS Publications Series* **33**, 207–212 (2008)

[7] J.S. Lawrence, G.R. Allen. M.C.B. Ashley, C. Bonner, S. Bradley, X. Cui, J. Everett, X. Feng, S. Hengst, J. Hu, Z. Jian, C.A. Kulesa, Y. Li, D. Luong-Van, A.M. Moore, C. Pennypacker, W. Qin, R. Riddle, Z. Shang, J.W.V. Storey, B. Sun, N. Suntzeff, N.F.H. Tothill, T. Travouillon, C.K. Walker, L. Wang, J. Yan, J. Yang, H. Yang, D. York, X. Yuan, X. Zhang, Z. Zhang, X. Zhou and Z. Zhu, "The PLATO Antarctic site testing observatory", *Proc. SPIE* **7012**, 701227-1–701227-12 (2008)

[8] A. Tokovinin, "Turbulence profiles from the scintillation of stars, planets and moon", *Workshop on Astronomical Site Evaluation (Eds. I. Cruz-González, J. Echevarría & D. Hiriart)* **31**, 61–70 (2007)

[9] J.W.V. Storey, M.C.B. Ashley, M.G. Burton, J.S. Lawrence, W. Saunders, "How can we understand the Antarctic Atmosphere?", *Proceedings from the International Conference Optical Turbulence Astronomy meets Meteorology 2008* in press (2008)

[10] C.S. Bonner, M.C.B. Ashley, J.S. Lawrence, J.W.V. Storey, D.M. Luong-Van, S.G. Bradley, "SNODAR: a new instrument to measure the height of the atmospheric boundary layer on the Antarctic plateau", *Proc. SPIE* **7014**, 70146I-1–70146I-7 (2008)

[11] C.S. Bonner, M.C.B. Ashley, J.S. Lawrence, D.M. Luong-Van, J.W.V. Storey, "Snodar II: Probing the atmospheric boundary layer on the Antarctic Plateau", *Proceedings from the International Conference Optical Turbulence Astronomy meets Meteorology 2008* in press (2008)

[12] H. Yang, G. Allen, M.C.B. Ashley, C.S. Bonner, S. Bradley, X. Cui, J.R. Everett,L. Feng, X. Gong, S. Hengst,J. Hu, Z. Jiang, C.A. Kulesa, J.S. Lawrence, Y. Li, D. Luong-Van, M.J. McCaughrean, A.M. Moore, C. Pennypacker, W. Qin, R. Riddle, Z. Shang, J.W.V. Storey, B. Sun, N. Suntzeff, N.F.H. Tothill, T. Travouillon, C.K. Walker, L. Wang, J. Yan, J. Yang, D. York, X. Yuan, X. Zhang, Z. Zhang, X. Zhou, Z. Zhu, "The PLATO Dome A Site-Testing Observatory: Instrumentation and First Results", *Publ. Astron. Soc. Pac.* **121**, 174–184 (2009)

[13] M.C.B. Ashley, G. Allen, C.S. Bonner, S.G. Bradley, X. Cui, J.R. Everett, L. Feng, X. Gong, S. Hengst, J. Hu, Z. Jiang, C.A. Kulesa, J.S. Lawrence, Y. Li, D.M. Luong-Van, M.J. McCaughrean, A.M. Moore, C. Pennypacker, W. Qin, R. Riddle, Z. Shang, J.W.V. Storey, B. Sun, N. Suntzeff, N.F.H. Tothill, T. Travouillon, C.K. Walker, L. Wang, J. Yan, H. Yang, J. Yang, D. York, X. Yuan, X. Zhang, Z. Zhang, X. Zhou, Z. Zhu, "PLATO—A robotic observatory for the Antarctic plateau", Proceedings of the 3rd ARENA Conference (Eds. N. Epchtein & L. Spinoglio), *EAS Publications Series*, in press (2009)

[14] A.N. Kolmogorov, "The local structure of turbulence in incompressible viscous fluid for very large Reynolds numbers", *Proc. R. Soc. London, Ser. A* **434**, 9–13 (1980)

[15] V.I Tatarskii, *The effects of the turbulent atmosphere on wave propagation*, Keter Press, Israle Jerusalem (1971)

[16] C.G. Little, "Acoustic methods for the remote probing of the lower atmosphere", *Proc. IEEE* **57**, 571–578 (1969)

[17] ISO 9613-1:1993 *Acoustics – Attenuation of sound during propagation outdoors – Part 1: Calculation of the absorption of sound by the atmosphere*, International Organization for Standardization, Geneva

[18] S.D. Danilov, A.E. Gur'yanov, M.A. Kallistratova, I.V. Petenko, S.P. Singal, D.R. Pahwa, B.S. Gera, "Acoustic calibration of sodars", *Meas. Sci. Technol.* **3**, 1001–1007 (1992)

[19] L.R. Dragonette, S. K. Numrich, L.J. Frank, "Calibration technique for acoustic scattering measurements", *J. Acoust. Soc. Am.* **69(4)**, 1186–1189 (1981)